Batteries & Supercaps

Research Article
doi.org/10.1002/batt.202200178

Chemistry Europe
European Chemical Societies Publishing

www.batteries-supercaps.org

Special Collection

Quadruply Fused Aromatic Heterocycles toward 4 V-Class Robust Organic Cathode-Active Materials

Kan Hatakeyama-Sato,*[a] Choitsu Go,[a] Tomoki Akahane,[a] Takahiro Kaseyama,[b] Takuji Yoshimoto,[b] and Kenichi Oyaizu*[a]

Quadruply fused aromatic heterocycles are examined as 4 V-class organic cathode-active materials. A newly synthesized dimethylfluoflavin-substituted polymer displays reversible charge/discharge at high potentials of 3.5 and 4.1 V (vs. Li/Li$^+$) as a cathode-active material for organic secondary batteries. The robust redox-active heterocycles enable the long cycle-life (>1000) while maintaining the high potential over 4 V. The linear polymer backbone and radical spin configuration in the heterocycles are the keys to enhancing the voltages and the cycle life.

Introduction

Organic redox-active molecules attract significant attention as the environmentally compatible electrode-active materials to replace the conventionally used metal oxide-based inorganic materials in the rechargeable batteries (e.g., lithium-ion batteries and redox-flow cells), and their potential application to various electrochemical devices such as solar cells is being explored.[1–5] The organic compounds are composed of inexhaustible light elements on earth (H, C, O, N, S, …), whereas rare or expensive metals are needed for conventional batteries (e.g., Co, Ni, Mn, and V). The various combinations of organic structures enable the flexible design of the electrodes, such as precise potential tuning, prompt charge/discharge properties, increased capacity, and even mechanical flexibility or stretchability.

In typical organic batteries, redox-active moieties are fixed on the electrodes, and their reversible electrochemical reactions can enable the facile charge transport and storage.[1,6–9] Even ultrafast rate performances (over 10^2 C, where ×C is a rate for fully charging/discharging cells in 1/x hours)) are often reported with soft materials, whereas many rigid inorganic materials tend to suffer from the larger resistances originating from the intercalation reactions during charge/discharge.[1,2,6,10]

Although the recent multi-electron redox design of organic molecules can offer higher charge/discharge capacities (>200 mAh/g) than conventional metal oxides (typically 100–200 mAh/g), their limited achievable redox potentials and stability have been problematic. The potentials of conventional redox-active molecules range from 1.5 to 3.7 V vs. Li/Li$^+$ (Figure 1a).[1,2,6,8] For instance, benzothiadiazole (ca. 1.5 V),[11] viologen (2 V),[12] anthraquinone (2 V),[13,14] phenazine (3.2 V),[15] triphenylamine (3.4 V),[16] phenothiazine (3.55 V),[17,18] and 2,2,6,6 tetramethylpiperidin-1-oxyl (TEMPO, 3.6 V)[1,7,19] have been studied extensively. The emerging concept of superlithiation would extend the limit down to 0 V vs. Li/Li$^+$.[20,21] On the other hand, increasing the potential by organic redox centers has not been fully successful, although reversible redox reactions of transition metals (e.g., Co, Ni, V, …) in inorganic metal oxides can offer over 4–5 V-class electrodes.

A new strategy is needed to break through the tradeoff between higher voltage and stability of organic cathode-active materials. Recently, some three-membered aromatic rings, such as thianthrene (4.1 V), carbazole (3.95 V), phenoxazine (3.7 V), were proposed as high-voltage organic cathodes (Figure 1a). The electron-withdrawing heteroatoms can shift the redox potentials during *p*-type redox reactions (i.e., becoming cations after oxidation). However, such compounds typically tend to suffer from rapid capacity decay (e.g., less than 100 cycles to reach 90% of the initial capacity) and lower Coulombic efficiency (<90%). Further, radical coupling reactions[22] at an early stage should be avoided for practical applications. The reactions will induce a significant loss of discharge capacity.

Here, we examined a series of quadruply fused aromatic heterocycles **1**–**5** for higher voltage organic cathode-active materials (Figure 1b). Introducing different heteroatoms (S or N) in aromatic rings increased the potentials up to 3.6–4.7 V. A promising cyclability (>90% capacity retention after 1000 cycles) was achieved by a dimethylfluoflavin polymer, where unfavorable capacity decay was suppressed by the rational polymeric and redox-center design (Figure 1c).

[a] Dr. K. Hatakeyama-Sato, C. Go, T. Akahane, Prof. K. Oyaizu
Department of Applied Chemistry
Waseda University
Tokyo 169-8555, Japan
E-mail: satokan@toki.waseda.jp
oyaizu@waseda.jp
[b] Dr. T. Kaseyama, Dr. T. Yoshimoto
Materials Research Laboratories, Frontier Material Research Department
Nissan Chemical Corporation
Chiba 274-0052, Japan

Supporting information for this article is available on the WWW under https://doi.org/10.1002/batt.202200178

Special Collection *An invited contribution to a Special Collection on Organic Batteries*

Research Article
doi.org/10.1002/batt.202200178
Chemistry Europe
European Chemical Societies Publishing

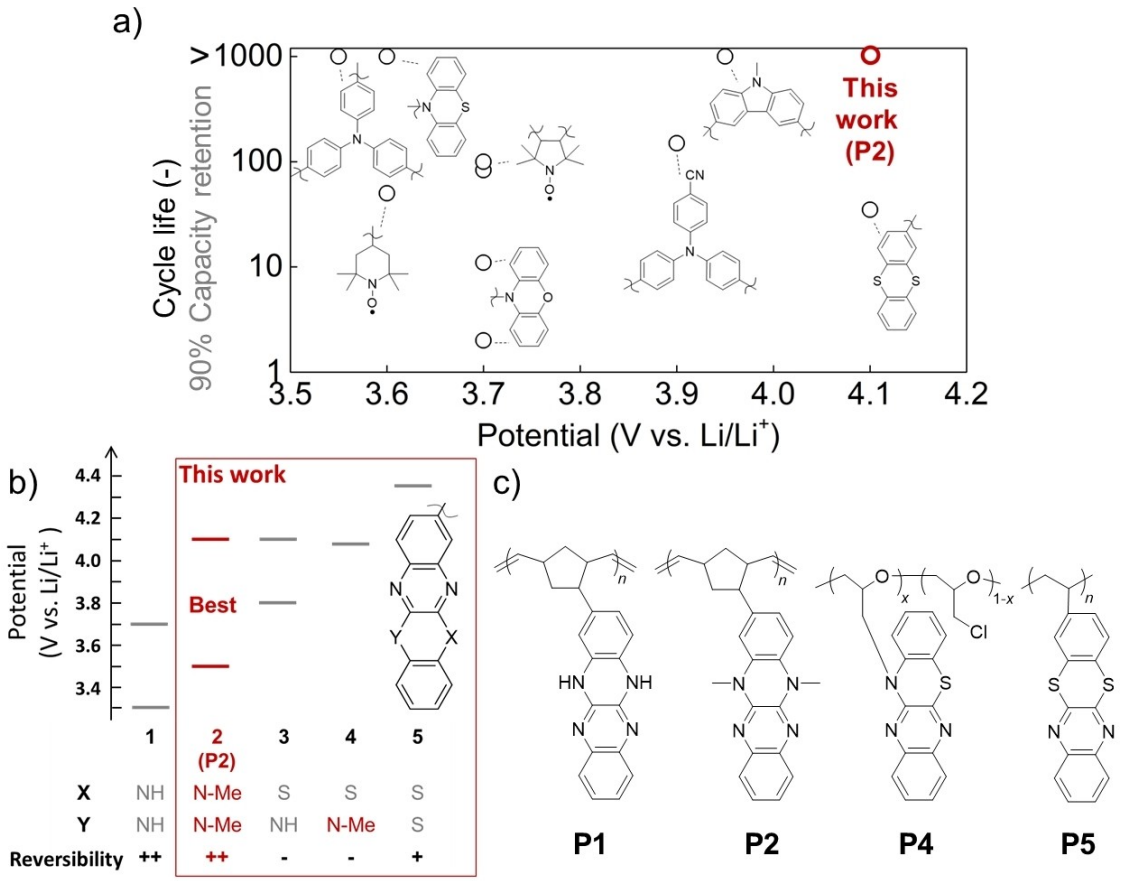

Figure 1. a) Comparison of redox-active centers focusing on redox potentials and cycle life.[16,17,23–30] b) Structures and redox potential of heterocycles examined in this study. c) Synthesized polymers.

Results and Discussion

There have been few studies on quadruply fused aromatic heterocycles as electrode-active materials, although their electrochemistry has been examined to show that some exhibited reversible responses in electrode reactions. We preliminary examined fluoflavin **1** and its polymer **P1**. The compound displayed reversible redox waves at 3.3 and 3.7 V vs. Li/Li^+, and a promising cycle-life over 100. This work aims to explore and reveal the chemistry of the quadruply fused cycles toward designing optimal cathode-active materials with high voltages.

Four types of aromatic cycles were designed, dimethylfluoflavin (**2**), and thiazino (**3**), *N*-methyl thiazino (**4**) and dithiino (**5**) derivatives of quinoxaline. Some molecules would also provide n-type redox reactions (becoming anions after reductions) by the nitrogen atoms in aromatic rings (around ca. 2–3 V vs. Li/Li^+).[6,31] In this work, we focused on *p*-type reactions to pursue 4 V-class cathodes, which has been challenging for organic materials.[6] The compounds were measured as the solutions in lithium-ion electrolytes by cyclic voltammetry (Figure 2a). Dimethylfluoflavin **2** displayed anodic peaks at $E_{pa} = 3.92$, 4.04 V and cathodic peaks at $E_{pc} = 3.64$, 3.84), corresponding to the reversible radical cation and dication (Figure 2b). The electron spin resonance (ESR) confirmed the two-step redox reactions, where characteristic spin peaks emerged in the radical cation state ($g = 2.0037$, Figure 2c).

The introduction of sulfur atoms to the rings enabled the operation of the molecules with higher redox potentials. The thiaziono compound **3** displayed reversible redox around 4.1 V, and the *N*-methyl thiazino ring **4** gave multiple redox around 3.9–4.5 V. The dithiino compound **5**, preliminarily examined by Kang et al.,[31] offered redox around 4.3 and 4.6 V. However, the reduction peak for the latter was small. The potentials were much higher than the corresponding three-membered ring, thianthrene (4.1 V), and most other organic cathode-active materials. The electron-withdrawing nitrogen atoms in the quadruply fused cycles increased the potentials, whereas the delocalization of electrons in the larger ring can contribute to enhanced stability.

We synthesized several new redox-active polymers containing the quadruply fused heterocycles (Scheme 1). A dimethylfluoflavin-substituted polynorbornene **P2** (151 mAh/g for two-electron redox per **2**) was synthesized via ring-opening metathesis polymerization. A Grubbs catalyst (3rd generation) was selected because it offered a high initiator efficiency and functional group tolerance against the redox-active fused rings.[32] The molecular weight was tuned facilely by changing the monomer/catalyst ratio because of the living-like property

Research Article
doi.org/10.1002/batt.202200178
Chemistry Europe
European Chemical Societies Publishing

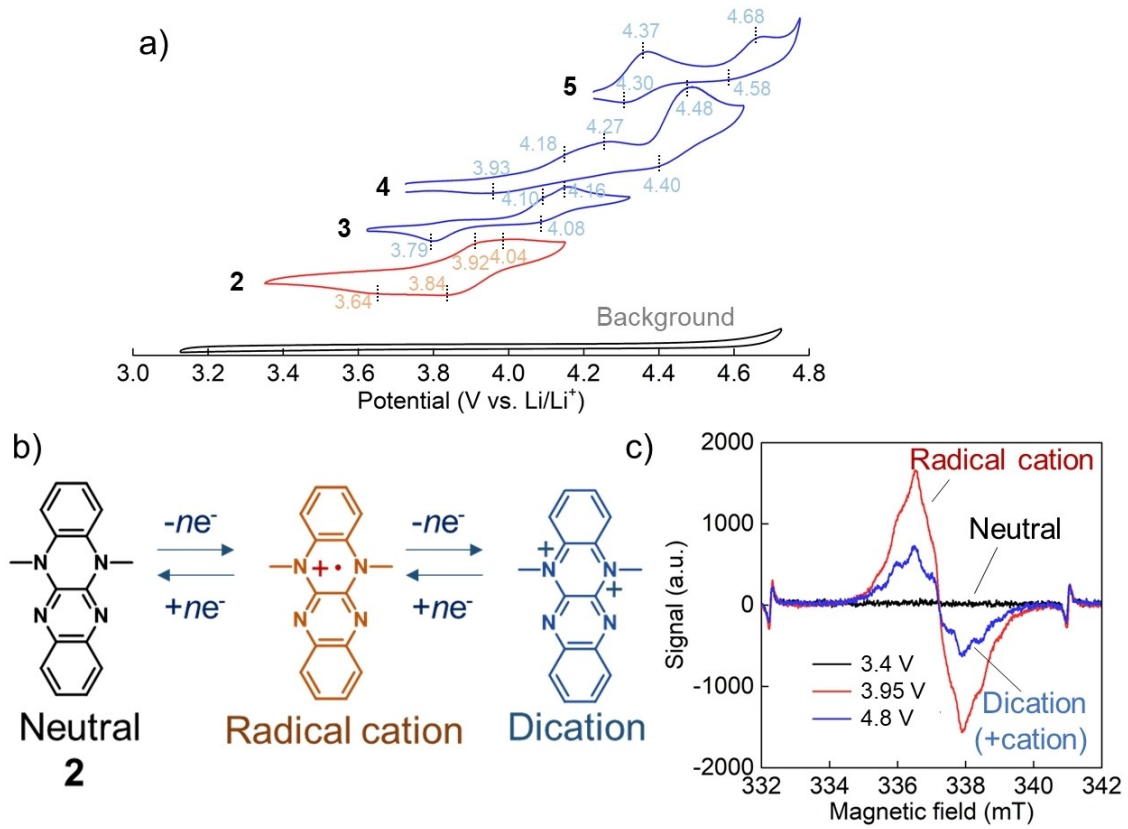

Figure 2. a) Cyclic voltammograms of **2**–**4** measured in 1 M $LiPF_6$ in ethylene carbonate/diethyl carbonate = 3/7 (v/v). The compounds were dissolved at 1–2 mM. The scan rate was 5 mV/s for **2** and 10 mV/s for the others. Absolute current values were scaled in the graph. b) Redox scheme of **2**. c) ESR spectra of **2** electrolyzed at different potentials. d) ESR spectra of the dimethylfluoflavin solution kept at different potentials (vs. Li/Li^+). No peak was found at the initial state (black line), and radical cation peaks emerged at 3.95 V. The peaks were attenuated at higher potentials by forming dications (blue line). It slightly remained because the formed dications could be reduced to cations at the counter electrode during the electrolysis.

of the polymerization (M_n of 8,300 to 30,000, Table S1).[32] Molecular weight is the most dominant factor to tune the solubility of the product. The sufficiently large molecular weight of **P2** ($M_w = 3.0\times10^4$, under 0.25 mol% catalyst) was enough to avoid unfavorable dissolution during the charge/discharge tests, whereas the polymer was soluble during the slurry preparation.

A vinyl polymer of dimethylfluoflavin **P2'** was also synthesized by radical polymerization for higher specific capacity (186 mAh/g). However, the poor solubility in reaction solvents (e.g., THF and CH_2Cl_2) limited the molecular weights up to only 2×10^3, as far as we examined. Facilely polymerizable norbornene units **P2** were suitable to tune molecular weight.

N-alkylthiazino (**P4**) and dithiino (**P5**) polymers were obtained as polyether and polyvinyl derivatives, respectively (Scheme 1). NH groups in **3** were reacted with polyepichlorohydrin ($M_w = 7.0\times10^5$) to yield **P4**. A vinyl polymer **P5** was synthesized by free radical polymerization ($M_w = 3.0\times10^4$). The polymers can offer specific capacities of 73 and 91 mAh/g, respectively, for one-electron reactions per unit (and twice for two-electron reactions).

The newly synthesized polymers exhibited remarkably high redox potentials over 4 V (Figure 3). A dimethylfluoflavin polymer **P2** afforded reversible redox around 3.5 and 4.1 V vs. Li/Li^+ during cyclic voltammetry (Figure 3a). The potentials differed from the solution states of **2** (3.8 and 3.9 V, Figure 2). Intermolecular interactions among the densely introduced redox units to polymer backbones could attribute to the potential shifts, as observed similarly with a standard fluoflavin polymer **P1**.[33] A new polymer **P2** displayed promising charge/discharge capability as a cathode. At a rate of 1 C, the specific charging capacity reached 122 mAh/g (81% against the theoretical capacity) and the Coulombic efficiency of over 90% (Figure 3b). Even at a higher rate of 30 C, the discharge capacity maintained around 90 mAh/g: the performance was one of the best for the high-voltage organic cathodes

Most importantly, an excellent cycle performance was observed with a dimethylfluoflavin polymer **P2** (Figure 3c, d). Even after repeating the charge/discharge at 10 C for 1000 cycles, the electrode maintained original redox plateaus and capacity over 90% against the initial. As far as we are concerned, realizing both high voltage (4.1 V) and long life (>1000 cycles) has not been achieved so far with organic electrodes (Figure 1).[23,24,34–36] We will discuss the key features to the stability in the later section.

Cyclic voltammograms of the sulfur-containing polymers, **P4** and **P5**, were also recorded to examine their basic electrochemical properties (Figure 3e, f). An *N*-alkylthiazino polymer

Research Article
doi.org/10.1002/batt.202200178
Chemistry Europe
European Chemical Societies Publishing

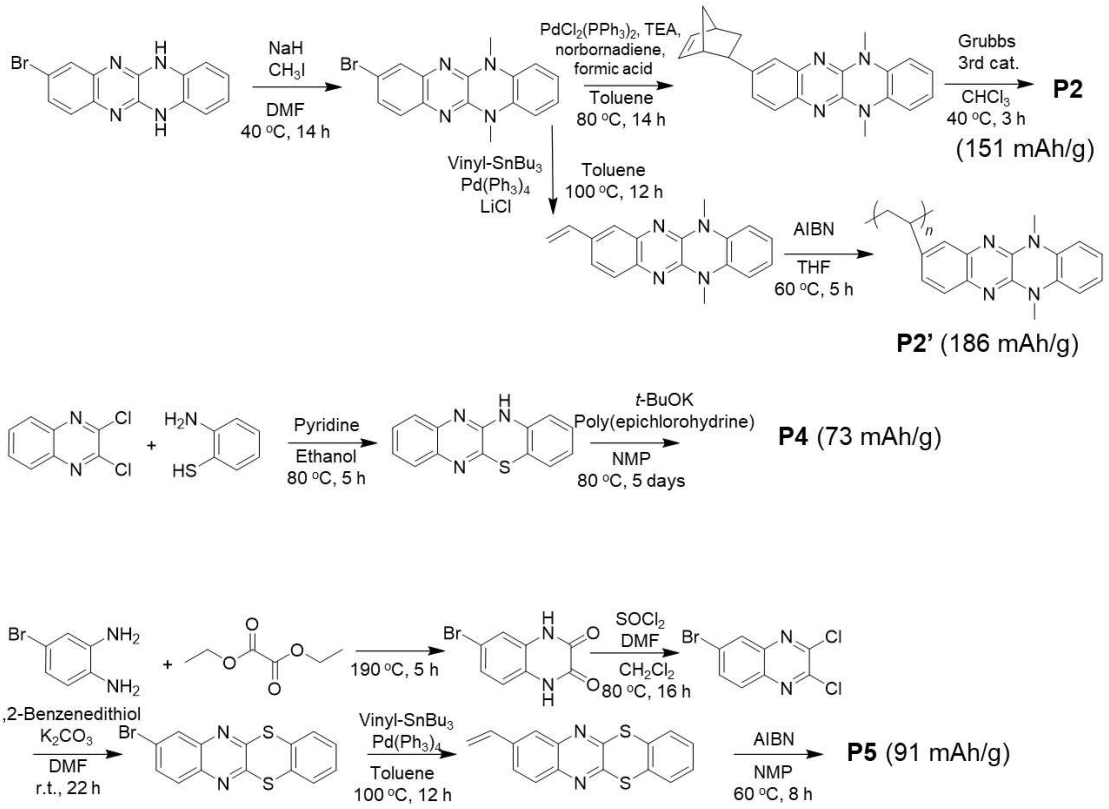

Scheme 1. Synthesis of **P2**, **P2'**, **P4**, and **P5**.

P4 displayed redox at around 4.0 V. However, the peaks faded rapidly along with repeated cycles, and new smaller peaks around 3.8 V emerged. The shift indicated the chemical deformation of the redox center **4** owing to the coupling reactions (Figure 4a). A dithiino polymer **P5** displayed a single redox peak couple at 4.3 V, which should be one of the highest among the organic active materials ever reported. Although the redox peaks faded gradually along with cycles, the absence of new redox peaks, in contrast to **P4**, indicated that carefully tuning the polymer structures and electrolytes could improve cyclability in future works.

We conducted basic density functional theory (DFT) calculations to rationalize the electrochemical properties of the examined aromatic rings (Figure 4). The observed redox potentials of **P1**, **P2**, **P4**, and **P5** were similar to the trend of HOMO of the corresponding monomeric species, **1**, **2**, **4**, and **5** (Figure S11). Between the two parameters, an approximated relationship of $E_{1/2} = -\mathrm{HOMO} + 2.9$ was obtained. The offset of 2.9 was determined manually; the value is affected by calculation errors of DFT, attributed to vacuum energy level, electrolyte effects, and other factors.[37,38]

The simple estimation yielded the potentials of 3.5, 3.4, 4.0, and 4.6 V for **1**, **2**, **4**, and **5**. The values matched the experimental first redox potentials of 3.3, 3.5, 4.1, and 4.4 V for **P1**, **P2**, **P4**, and **P5**, respectively. The more significant electron-withdrawing properties of sulfur atoms than nitrogens increased the potentials of **P4** and **P5** from **P2**. The DFT calculation predicted a higher redox potential of **P1** (3.5 V) than **P2** (3.4 V) certainly because of the electron-donating effects of methyl groups. The contradiction against the experimental results (**P1**: 3.3 and **P2**: 3.5 V) may be explained by proton-coupled redox reactions of **P1** and other electrostatic interactions among the redox sites and electrolytes.[6,33,39,40]

Mulliken spin densities for the radical cations of **2**, **4**, and **5** were visualized to rationalize the electrochemical stability of the molecules (Figures 4 and S12). In dimethylfluoflavin **2**, the most robust compound in this study, radical spins were located mainly on nitrogen atoms connected to methyl groups. According to the calculation, only the two atoms in the molecule exceeded the Mulliken spin density of 0.1. The localization indicated that redox reactions were induced mostly at the N,N'-dimethylphenazine unit, not quinoxaline in the quadruply fused cycles. The nitrogen atoms were thoroughly surrounded by carbon atoms of aromatic rings and methyl groups, sterically protecting radicals and thus enhancing stability.[41] The spin densities did not change drastically by the calculation with lithium salts, indicating that the properties were mainly attributed to the geometry of the molecules, not electrolytes (Figure S12).

In contrast to **2**, spins were distributed on sulfur (density of 0.26), sp^3 nitrogen (0.29), and several carbon atoms (ca. 0.1) in the *N*-methylthiazino compound **4**. The asymmetrical molecular geometry generated the active radical carbons exposed to the outside environment. The sulfur atom also lacked sterical protective groups. In the case of the dithiino derivative **5**, two active sulfur and two carbon atoms were exposed to the

Research Article
doi.org/10.1002/batt.202200178
Chemistry Europe
European Chemical Societies Publishing

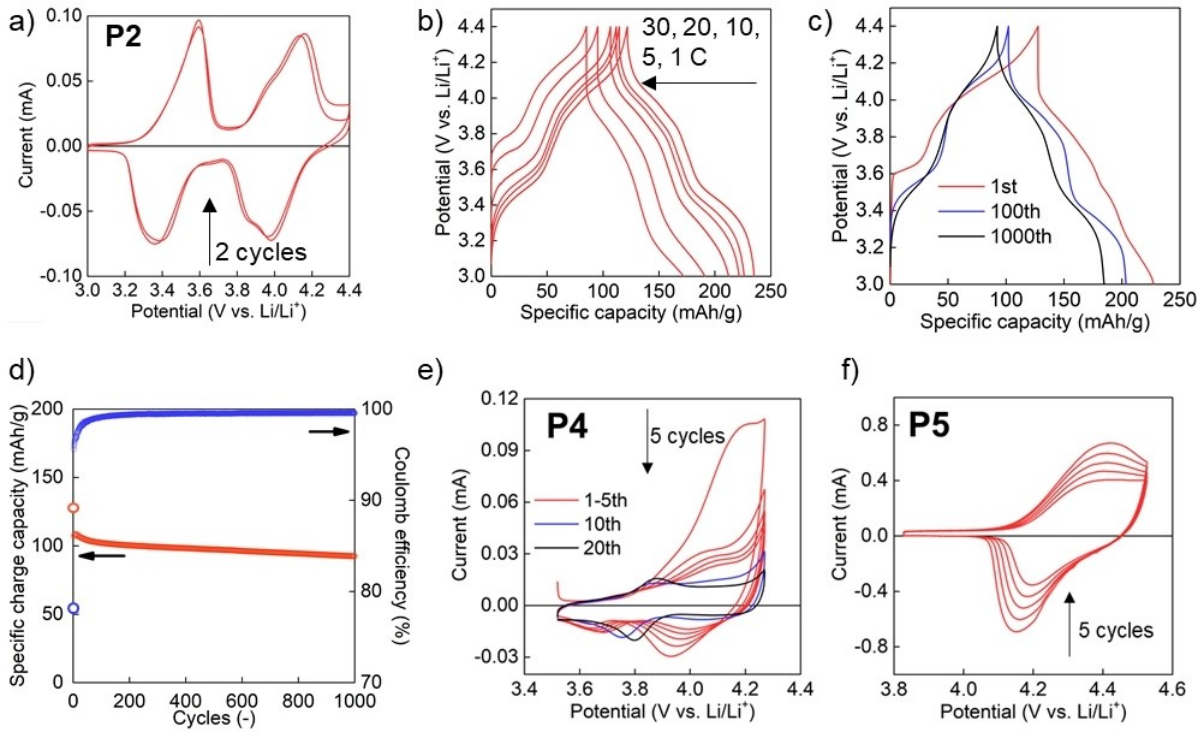

Figure 3. a) Cyclic voltammogram of a rechargeable battery using a **P1**/vapor-grown carbon fiber/polyvinylidene difluoride = 1/8/1 composite electrode as a cathode. Lithium foil was used as an anode. The scan rate was 1 mV/s. b) Charge/discharge curves of the cell with different charge/discharge rates (1, 5, 10, 20, and 30 C). c) Charge/discharge curves at different cycles, measured at 10 C. d) Discharge capacity and Coulombic efficiency for the cycle test. e) Cyclic voltammogram of the **P4** composite electrode (scan rate: 1 mV/s). f) Cyclic voltammogram of the **P5** composite electrode (scanned rate 5 mV/s). Measurements were conducted using an $Ag/AgNO_3$ reference electrode for e) and f).

outside. Those unprotected radical atoms should have induced side reactions with neighboring electrolytes and redox units.

The electrochemical cycle stability can also be explained by organic reactions (Figure S13). A radical cation of dimethylfluoflavin has two resonance structures of *N*-centered radicals. Kinetically, nitrogen atoms existing in conjugated structures and neighboring protective carbon atoms are reported to be electrochemically robust:[6,16,41] this was consistent with the excellent stability of **2**. Its dicationic state also satisfies the Hückel rule of aromaticity, strongly stabilizing the charged structures ($4n+2=18$, Figure 2b).

In contrast to **2**, carbon radicals in **4**, emerging in resonance structures, should be highly reactive. Electrochemical coupling reactions by carbon radicals are widely observed with carbazoles, triphenylamines, and other asymmetrical heterocycles, regardless of the types of electrolytes (Figure 4b).[2,9,16,22,24,26,28,34] The current decay and potential shift of **P4** after the repeated sweeps can be explained by such coupling reactions.

Sulfur radicals in **4** and **5** should be more stable than carbons.[22] However, sulfur radicals in aromatic rings (e.g., thianthrene) are known to couple with aromatic rings and other molecules.[42,43] Organic cathodes with sulfur radicals as the redox centers tend to display insufficient cyclability, as observed with **P5**.[23,31,35] Their details have been unclear,[23,31,35] but their decaying process should be elucidated to improve cyclability for practical applications in future works.

Finally, we compared dimethylfluoflavin (**2**) with a popular redox-active center, *N*,*N*′-dimethylphenazine. The molecule can also provide redox at around 3.3 and 4.1 V (vs. Li/Li^+).[15,36,44,45] Although the compact structure is favored for higher energy density, dimethylphenazine typically tends to suffer from low Coulombic efficiency (< 90%) at early cycles and often inferior cyclability than our new polymer **P2**.[15,36,44,45] The significant reasons are suspected to be the demethylation of the dication[46] or dissolution into electrolytes.[45]

In addition to the high molecular weight of the polymer, cyclability may be explained by the structure of aromatic rings in the oxidized states. Estimated geometry for the cations of dimethylfluoflavin and dimethylphenazine may explain the advantage of the quadruply fused cycles (Figure 5). Both compounds had bent structures along the line of two sp^3 nitrogen atoms (around 150°–160°). In the cationic states, the two compounds became more planar (179° and 164° for dimethylfluoflavin and dimethylphenazine, respectively). Almost planar geometry was obtained with dimethylfluoflavin because of the delocalized conjugated structure in the quadruply fused cycles. The flatness should be essential to achieve conjugation for higher chemical stability and also suppress the unfavorable dissolution of the active materials into electrolytes. Flat aromatic rings can benefit $\pi-\pi$ interactions between the redox units, as a kind of physical cross-linking,[39] whereas bent dimethylphenazines[45] were reported as highly soluble.

Research Article
doi.org/10.1002/batt.202200178
Chemistry Europe
European Chemical Societies Publishing

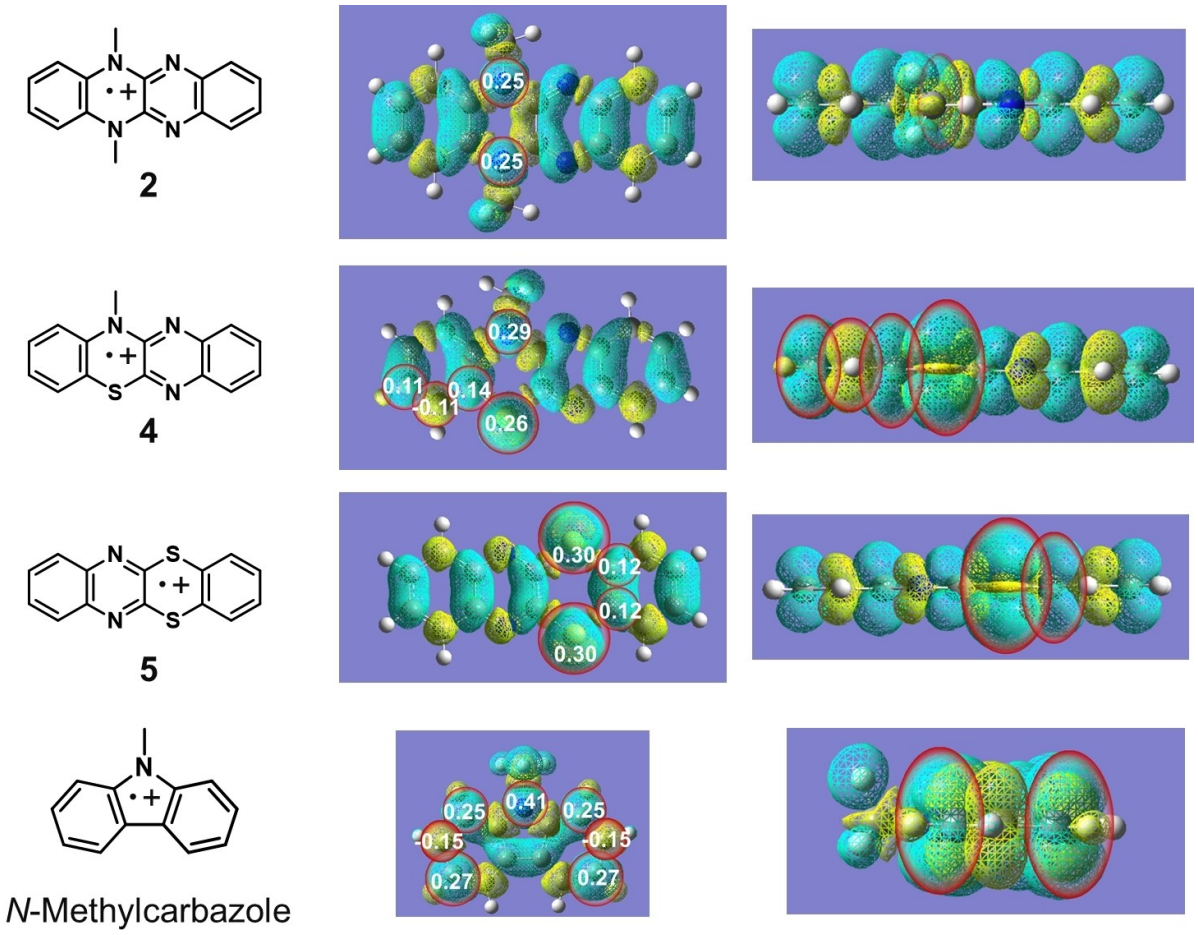

Figure 4. Estimated spin states of the aromatic hetero ring in the charged states (radical cations of **2**, **4**, **5**, and *N*-methylcarbazole). Milliken spin density and orbital surfaces are shown. Atoms and orbitals with higher spin densities (absolute value of >0.1) are marked red. Spin densities of all atoms and calculation results with the existence of salts are provided in Figure S12.

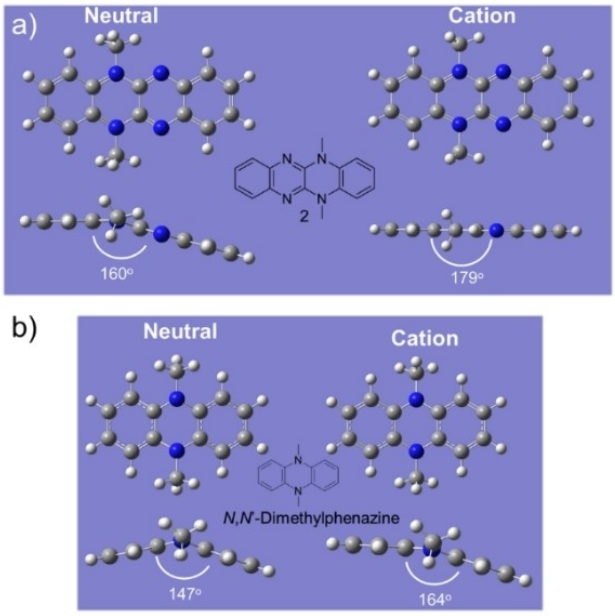

Figure 5. Estimated geometry of the redox species in the neutral and cationic states. a) **2**. b) Dimethylphenazine.

Conclusion

A robust dimethylfluoflavin polymer was synthesized as organic cathode-active material. The new polymer displayed one of the highest redox potentials (3.5 and 4.1 V vs. Li/Li^+) while maintaining excellent redox durability (>1000 charge/discharge cycles). Other quadruply fused aromatic heterocycles, thiazino, *N*-methyl thiazino, and dithiino derivatives of quinoxaline, also exhibited high potentials (3.6–4.7 V). DFT calculations rationalized their stability. Design of protected radical species and planar geometry was essential to avoid side reactions and unfavorable dissolutions. Further theoretical and spectroscopic analysis of molecular and electrode structures will be needed to reveal their redox reactions, including side reactions. We are pursuing an ideal molecular strategy by balancing high potentials (>4 V vs. Li/Li^+) and cyclability for the practical application of organic electrode-active materials.

Experimental Section

Electrochemical measurements

Cyclic voltammogram of dissolved species: A conventional potentiostat (BAS ALS 660D) was used for standard electrochemical measurements with a three-electrode system. A platinum coil and an $Ag/AgNO_3$ wire were used as the counter and reference electrodes. A glassy carbon electrode was employed as a working electrode. 1 M $LiPF_6$ in ethylene carbonate (EC)/diethyl carbonate (DEC) = 3/7 (v/v) was used as the electrolyte unless otherwise noted. Potentials were calibrated using ferrocene and converted against Li/Li^+ assuming $E_{1/2} = 3.2$ V vs. Li/Li^+ for ferrocene.

Electron spin resonance spectroscopy: Electron spin resonance (ESR) spectroscopy was conducted by JEOL JESTE200. For ESR, 1 mM dimethylfluoflavin solution of 0.1 M tetrabutylammonium hexafluorophosphate in dichloromethane was prepared. Then, the constant potentials were applied to yield the neutral, cation, and dication species. A three-electrode system was employed for the electrolysis using an Ag wire as the reference.

Electrode preparation: Carbon composite electrodes were prepared by mixing the cathode-active polymer, vapor-grown carbon fiber (VGCF, Showa Denko Co.), and polyvinylidene difluoride (PVdF, Kureha Co.). After dissolving the active material and PVdF in *N*-methylpyrrolidone, VGCF was added and mixed using a mortar. Then, the slurry was cast on a carbon-coated aluminum foil (MTI Co.). The weight ratio in the composite was active material/VGCF/PVdF = 1/8/1 (wt/wt/wt). The prepared electrodes had a typical areal weight of 3 mg/cm^2, a thickness of 40 μm, and a density of 0.8 g/cm^3. The loading amount of active materials was small because this study focused on the redox capability of active materials. Reducing the number of conductive carbons would require special conductive agents and preparation methods because of the insufficient conductivity of non-conjugated polymers).[10] Specific capacity (value per weight of active materials) is discussed in this paper.

Cell fabrication: Lithium foil was used as the anode, and Celgard #2400 was used as the separator. Lithium batteries were fabricated in an argon-filled glove box. The cells were tested by a conventional battery charge/discharge system (HJ1001SD8, Hokuto Denko Co.).

Other measurements

Molecular weights of polymers were measured by gel permeation chromatography with chloroform eluent and polystyrene standards.

Density functional theory (DFT) calculation

Calculations were conducted using Gaussian16. Single molecular structures without solvent molecules were calculated unless noted otherwise. Initially, geometry was optimized by PM6 level. Then, structure optimization and spin density calculation were conducted with B3LYP/6-31 + g(d′). In Figure 4, one-electron oxidized states (radical cations) of the molecules were calculated. Mulliken spin charges on atoms and orbital surfaces for spin density were visualized in the figures (blue: positive spin and yellow: negative). In Figure S12, calculations were also conducted with the existence of a $LiPF_6$ molecule under a solvation model based on density (SMD) model for more precise estimation. Properties of a conventional molecule, acetonitrile, were conveniently employed for the dielectric properties for SMD instead of the unfamiliar mixture of EC/DEC for the model. Neutral and radical cation states were calculated in Figure 5 (without salt or SMD). In Figure S11, HOMO levels were simply estimated from the orbital energies of the molecules in neutral states (i.e., Koopmans' theorem).[37]

Acknowledgements

This work was partially supported by Grants-in-Aid for Scientific Research (Nos. 21H04695, 18H05515, 20H05298, 22H04623, and 21H02017) from MEXT, Japan. The work was partially supported by supported by JST FOREST Program (Grant Number JPMJFR213V, Japan) the Research Institute for Science and Engineering, Waseda University.

Conflict of Interest

The authors declare no conflict of interest.

Data Availability Statement

The data that support the findings of this study are available from the corresponding author upon reasonable request.

Keywords: high-voltage organic cathodes · lithium battery · organic cathode-active material

[1] S. Y. Wang, A. D. Easley, J. Lutkenhaus, *ACS Macro Lett.* **2020**, *9*, 358–370.
[2] A. Saal, T. Hagemann, U. S. Schubert, *Adv. Energy Mater.* **2020**, *11*, 2001984.
[3] K. Hatakeyama-Sato, T. Tezuka, R. Ichinoi, S. Matsumono, K. Sadakuni, K. Oyaizu, *ChemSusChem* **2020**, *13*, 2443–2448.
[4] Y. Xie, K. Zhang, Y. Yamauchi, K. Oyaizu, Z. Jia, *Mater. Horiz.* **2021**, *8*, 803–829.
[5] T. P. Nguyen, A. D. Easley, N. Kang, S. Khan, S. M. Lim, Y. H. Rezenom, S. Wang, D. K. Tran, J. Fan, R. A. Letteri, X. He, L. Su, C. H. Yu, J. L. Lutkenhaus, K. L. Wooley, *Nature* **2021**, *593*, 61–66.
[6] J. J. Shea, C. Luo, *ACS Appl. Mater. Interfaces* **2020**, *12*, 5361–5380.
[7] K. Sato, R. Ichinoi, R. Mizukami, T. Serikawa, Y. Sasaki, J. Lutkenhaus, H. Nishide, K. Oyaizu, *J. Am. Chem. Soc.* **2018**, *140*, 1049–1056.
[8] Q. Zhao, Z. Zhu, J. Chen, *Adv. Mater.* **2017**, *29*, 1607007.
[9] P. Taranekar, T. Fulghum, D. Patton, R. Ponnapati, G. Clyde, R. Advincula, *J. Am. Chem. Soc.* **2007**, *129*, 12537–12548.
[10] K. Hatakeyama-Sato, H. Wakamatsu, R. Katagiri, K. Oyaizu, H. Nishide, *Adv. Mater.* **2018**, *30*, e1800900.
[11] W. Duan, J. Huang, J. A. Kowalski, I. A. Shkrob, M. Vijayakumar, E. Walter, B. Pan, Z. Yang, J. D. Milshtein, B. Li, C. Liao, Z. Zhang, W. Wang, J. Liu, J. S. Moore, F. R. Brushett, L. Zhang, X. Wei, *ACS Energy Lett.* **2017**, *2*, 1156–1161.
[12] A. Ghosh, S. Mitra, *RSC Adv.* **2015**, *5*, 105632–105635.
[13] I. Gomez, O. Leonet, J. A. Blazquez, H. J. Grande, D. Mecerreyes, *ACS Macro Lett.* **2018**, *7*, 419–424.
[14] Z. Zhu, M. Hong, D. Guo, J. Shi, Z. Tao, J. Chen, *J. Am. Chem. Soc.* **2014**, *136*, 16461–16464.
[15] M. Lee, J. Hong, B. Lee, K. Ku, S. Lee, C. B. Park, K. Kang, *Green Chem.* **2017**, *19*, 2980–2985.
[16] K. Yamamoto, D. Suemasa, K. Masuda, K. Aita, T. Endo, *ACS Appl. Mater. Interfaces* **2018**, *10*, 6346–6353.
[17] F. Otteny, M. Kolek, J. Becking, M. Winter, P. Bieker, B. Esser, *Adv. Energy Mater.* **2018**, *8*, 1802151.
[18] V. Perner, D. Diddens, F. Otteny, V. Kupers, P. Bieker, B. Esser, M. Winter, M. Kolek, *ACS Appl. Mater. Interfaces* **2021**, *13*, 12442–12453.

[19] S. Perticarari, E. Grange, T. Doizy, Y. Pellegrin, E. Quarez, K. Oyaizu, A. J. Fernandez-Ropero, D. Guyomard, P. Poizot, F. Odobel, J. Gaubicher, *Chem. Mater.* **2019**, *31*, 1869–1880.
[20] H. Q. Yang, S. W. Liu, L. H. Cao, S. H. Jiang, H. Q. Hou, *J. Mater. Chem. A* **2018**, *6*, 21216–21224.
[21] H. Numazawa, Y. Igarashi, K. Sato, H. Imai, Y. Oaki, *Adv. Theory Simul.* **2019**, *2*, 1900130.
[22] Y. Yuan, J. Yang, A. Lei, *Chem. Soc. Rev.* **2021**, *50*, 10058–10086.
[23] M. E. Speer, M. Kolek, J. J. Jassoy, J. Heine, M. Winter, P. M. Bieker, B. Esser, *Chem. Commun.* **2015**, *51*, 15261–15264.
[24] K. Lee, I. E. Serdiuk, G. Kwon, D. J. Min, K. Kang, S. Y. Park, J. E. Kwon, *Energy Environ. Sci.* **2020**, *13*, 4142–4156.
[25] K. Nakahara, K. Oyaizu, H. Nishide, *Chem. Lett.* **2011**, *40*, 222–227.
[26] Y. Zhang, P. P. Gao, X. Y. Guo, H. Chen, R. Q. Zhang, Y. Du, B. F. Wang, H. S. Yang, *RSC Adv.* **2020**, *10*, 16732–16736.
[27] K. A. Hansen, J. Nerkar, K. Thomas, S. E. Bottle, A. P. O'Mullane, P. C. Talbot, J. P. Blinco, *ACS Appl. Mater. Interfaces* **2018**, *10*, 7982–7988.
[28] L. M. Zhu, X. Y. Cao, *Mater. Lett.* **2015**, *150*, 16–19.
[29] C. Zhao, Z. Chen, W. Wang, P. Xiong, B. Li, M. Li, J. Yang, Y. Xu, *Angew. Chem. Int. Ed.* **2020**, *59*, 11992–11998; *Angew. Chem.* **2020**, *132*, 12090–12096.
[30] K. Oyaizu, T. Kawamoto, T. Suga, H. Nishide, *Macromolecules* **2010**, *43*, 10382–10389.
[31] J. Kim, H. Kim, S. Lee, G. Kwon, T. Kang, H. Park, O. Tamwattana, Y. Ko, D. Lee, K. Kang, *J. Mater. Chem. A* **2021**, *9*, 14485–14494.
[32] G. C. Vougioukalakis, R. H. Grubbs, *Chem. Rev.* **2010**, *110*, 1746–1787.
[33] K. Hatakeyama-Sato, T. Akahane, C. Go, T. Kaseyama, T. Yoshimoto, K. Oyaizu, *ACS Energy Lett.* **2020**, *5*, 1712–1717.
[34] J. T. Ren, X. X. Wang, H. Liu, Y. M. Hu, X. Q. Zhang, T. Masuda, *React. Funct. Polym.* **2020**, *146*, 104365.
[35] K. Hatakeyama-Sato, T. Masui, T. Serikawa, Y. Sasaki, W. Choi, S. G. Doo, H. Nishide, K. Oyaizu, *ACS Appl. Energ. Mater.* **2019**, *2*, 6375–6382.
[36] G. L. Dai, X. L. Wang, Y. M. Qian, Z. H. Niu, X. Zhu, J. Ye, Y. Zhao, X. H. Zhang, *Energy Storage Mater.* **2019**, *16*, 236–242.
[37] J. Conradie, *J. Phys. Conf. Ser.* **2015**, *633*, 012045.
[38] D. D. Mendez-Hernandez, P. Tarakeshwar, D. Gust, T. A. Moore, A. L. Moore, V. Mujica, *J. Mol. Model.* **2013**, *19*, 2845–2848.
[39] M. Kolek, F. Otteny, P. Schmidt, C. Mück-Lichtenfeld, C. Einholz, J. Becking, E. Schleicher, M. Winter, P. Bieker, B. Esser, *Energy Environ. Sci.* **2017**, *10*, 2334–2341.
[40] A. Gallastegui, D. Minudri, N. Casado, N. Goujon, F. Ruipérez, N. Patil, C. Detrembleur, R. Marcilla, D. Mecerreyes, *Sustain. Energy Fuels.* **2020**, *4*, 3934–3942.
[41] B. Tang, J. Zhao, J. F. Xu, X. Zhang, *Chem. Sci.* **2020**, *11*, 1192–1204.
[42] H. J. Shine, J. J. Silber, *J. Org. Chem.* **2002**, *36*, 2923–2926.
[43] F. Berger, M. B. Plutschack, J. Riegger, W. Yu, S. Speicher, M. Ho, N. Frank, T. Ritter, *Nature* **2019**, *567*, 223–228.
[44] G. Kwon, S. Lee, J. Hwang, H. S. Shim, B. Lee, M. H. Lee, Y. Ko, S. K. Jung, K. Ku, J. Hong, K. Kang, *Joule* **2018**, *2*, 1771–1782.
[45] C. N. Gannett, B. M. Peterson, L. Shen, J. Seok, B. P. Fors, H. D. Abruna, *ChemSusChem* **2020**, *13*, 2428–2435.
[46] R. F. Nelson, D. W. Leedy, E. T. Seo, R. N. Adams, *Fresenius Z. Anal. Chem.* **1966**, *224*, 184–196.

Manuscript received: April 16, 2022
Accepted manuscript online: April 27, 2022
Version of record online: May 19, 2022